

Compact Tri-Band Dual-Polarized Planar Monopole Antenna with Asymmetrical Ground Plane and Loaded Stub

Ming-Tao Tan, Bing-Zhong Wang*, and Zhi-Min Zhang

Abstract—This paper presents a compact tri-band dual-polarized planar monopole antenna, which is linearly polarized in the lower and middle bands and circularly polarized in the higher band. The antenna is printed on a substrate with an asymmetrical ground plane and a loaded vertical stub. The vertical stub and asymmetrical ground plane are mainly used to make the antenna obtain circular polarization performance in the higher band. The antenna has been built and tested. Its measured 10-dB impedance bandwidths are 2.39–2.54 GHz, 3.38–4.12 GHz, and 4.57–6.04 GHz, which can fully cover all the 2.4/5.2/5.8 GHz WLAN bands, all the 2.4/5.5 GHz Wi-Fi bands, and 3.5/5.5 GHz WiMAX bands. In the higher band, the measured 3-dB axial-ratio bandwidth is 5.4–5.83 GHz.

1. INTRODUCTION

With the development of modern communication systems and technologies such as Wireless Fidelity (Wi-Fi), Wireless Local Area Network (WLAN), and Worldwide Interoperability for Microwave Access (WiMAX), the demand for antennas with compact size, multiband operation is increasing. Multi-band antennas with the same polarization in all bands are often realized using microstrip antennas [1], monopole antennas [2, 3], slot antennas [4], reconfigurable antennas [5], etc. Multi-band antennas with dual polarization performance have also been realized [6–9]. In [6], a triangular microstrip antenna realizes dual-band dual-polarized function. In [7], a stacked-patch dual-polarized antenna is designed for triple-band handheld terminals. In [8], three corners of a coaxial probe-fed sector shaped patch antenna are truncated to realize tri-band dual-polarized performance. In [9], a microstrip patch antenna with triple-band and dual-polarized performance is presented. Although those antennas have multi-band dual-polarized performance, the dimensions of the antennas are relatively large and the structures of the antennas are relatively complicated.

In this paper, a compact coplanar waveguide(CPW)-fed tri-band dual-polarized planar monopole antenna is presented. Compared with the design in [3], the geometrical structure of the proposed antenna is somewhat similar, but the operation mechanism is different and dual polarization is obtained. The antenna is printed on a substrate with an asymmetrical ground plane and a loaded vertical stub. The vertical stub is mainly used for obtaining circular polarization (CP) performance in the higher band and the asymmetrical ground plane mainly for improving CP and especially impedance match performance. It has the measured 10-dB impedance bandwidths of 150 MHz in the lower band (2.39–2.54 GHz), 740 MHz in the middle band (3.38–4.12 GHz), and 1470 MHz in the higher band (4.57–6.04 GHz) to fully cover all the 2.4/5.2/5.8 GHz WLAN bands, all the 2.4/5.5 GHz Wi-Fi bands, and 3.5/5.5 GHz WiMAX bands. Its measured 3-dB axial-ratio (AR) bandwidth is 430 MHz in the higher band. Details of the antenna design and the simulated and measured results are presented and discussed.

Received 20 December 2015, Accepted 14 January 2016, Scheduled 21 January 2016

* Corresponding author: Bing-Zhong Wang (bzwang@uestc.edu.cn).

The authors are with the Institute of Applied Physics, University of Electronic Science and Technology of China, Chengdu 610054, China.

2. ANTENNA DESIGN

2.1. Antenna Configuration

Figure 1(a) shows the geometrical configuration of the proposed antenna. Figure 1(b) shows the fabricated antenna. The antenna uses an inexpensive FR4-epoxy substrate with a thickness of 1.6 mm, a relative permittivity of 4.6, and a loss tangent of 0.02. One side of the FR4 dielectric substrate is covered with an etched metal layer, while the other side without metallization. The antenna is fed by a 50- Ω CPW transmission line with a signal strip width of 3.6 mm and a gap distance of 0.5 mm between the signal strip and the ground plane.

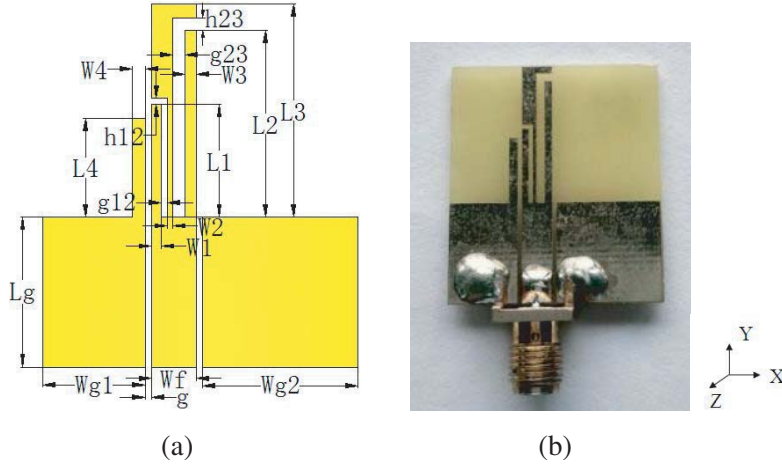


Figure 1. (a) Configuration of the proposed antenna; (b) fabricated antenna.

The width of the antenna radiator is the same as that of the signal strip of the CPW feedline. Two inverted-L slots are etched on the radiator, and the radiator is divided into three different parts for tri-band operation. A vertical stub on the left-half ground plane is mainly used to realize CP in the higher band and the asymmetrical ground plane is mainly used to improve CP and especially impedance match performance. Geometric parameters of the proposed antenna are listed in Table 1. The antenna design and optimization are carried out using the commercial software High Frequency Structure Simulator (HFSS).

Table 1. Geometric parameters of the proposed antenna.

Parameter	Value (mm)	Parameter	Value (mm)
Wf	3.6	$W1$	0.8
g	0.5	$W2$	0.3
$Wg1$	8.25	$W3$	0.9
$Wg2$	12.5	$W4$	1
Lg	12	$h12$	0.5
$L1$	9	$h23$	1
$L2$	14.9	$g12$	0.5
$L3$	17	$g23$	1
$L4$	7.9		

2.2. Design Evolution

Figure 2 shows design evolution of the antenna, and their corresponding simulated S_{11} are shown in Figure 3. The ground plane of Prototype A is symmetrical. Its simulated 10-dB impedance bandwidths are 2.39–2.43 GHz, 3.20–3.73 GHz, and 4.81–5.72 GHz. Figure 4 gives the simulated variations of AR against frequency of Prototypes A and B, and the proposed antenna in the $+z$ axis direction. Prototype A is linearly polarized in its operating bands.

In order to realize CP in the operating bands, a vertical stub is added on the left-half ground plane, as shown in Prototype B. The vertical stub affects the impedance match performance of Prototype B, especially at the higher frequencies. Prototype B has the simulated 10-dB impedance bandwidths: 2.4–2.48 GHz, 2.94–3.96 GHz, and 5.6–6.1 GHz. The CP performance of Prototype B is much better than that of Prototype A and still needs to be further improved.

In order to further improve tri-band and CP performance, we increase the width of the right-half ground plane of the CPW in Prototype B, and the proposed antenna is formed. Its simulated 10-dB impedance bandwidths are 2.39–2.48 GHz, 3.37–4.05 GHz, and 4.6–6.26 GHz, which can cover all the 2.4/5.2/5.8 GHz WLAN bands, all the 2.4/5.5 GHz Wi-Fi bands, and 3.5/5.5 GHz WiMAX bands. The proposed antenna has a better impedance match performance than Prototype B. The reason is that the effect of the asymmetrical ground plane on impedance match can balance out the effect of the vertical stub on impedance match. The simulated 3-dB AR bandwidth of the proposed antenna is from 5.46 to 5.93 GHz.

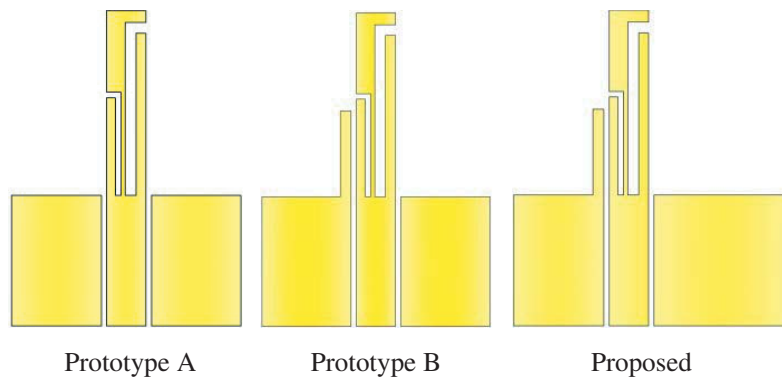


Figure 2. Design evolution of the proposed antenna.

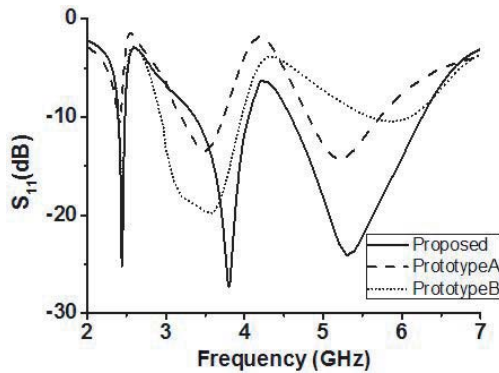


Figure 3. Simulated S_{11} of antennas involved in Figure 2.

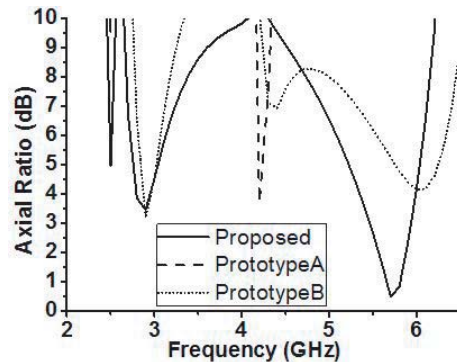


Figure 4. Simulated AR of various antennas involved in Figure 2.

2.3. Analysis of Current Distribution

In order to clarify the tri-band operation mechanism, the simulated surface current density distribution on the proposed antenna at 2.45, 3.5, and 5.5 GHz is shown in Figure 5. Surface current density is largest along the middle radiating element at 2.45 GHz, which shows that the middle element produces resonance and is the major radiating one at the lower frequencies. The length $L3$ of the middle element is approximately a quarter guided-wavelength at 2.45 GHz. At 3.5 GHz, surface current density is largest along the right radiating element, which indicates that the right element is the major radiating one at the middle frequencies. The length $L2$ of the right element is approximately a quarter guided-wavelength at 3.5 GHz. At 5.5 GHz, the left radiating element has strongest surface current density, which indicates that the left element contributes most to resonance in the higher band. The length $L1$ of the left element is approximately a quarter guided-wavelength at 5.5 GHz.

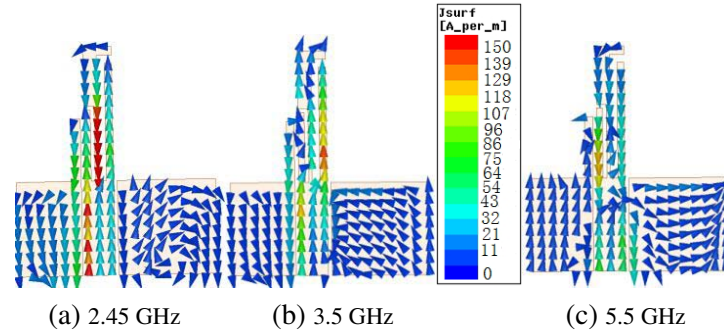


Figure 5. Simulated surface current density distribution on the proposed antenna at (a) 2.45 GHz, (b) 3.5 GHz, and (c) 5.5 GHz.

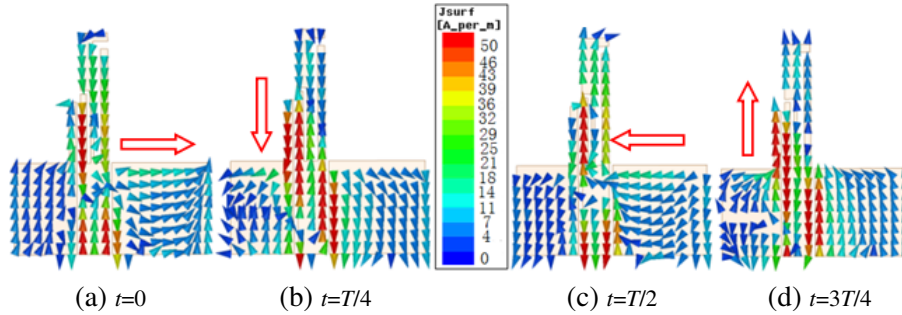


Figure 6. Simulated surface current density distribution on the proposed antenna at 5.6 GHz.

In order to explain the CP operation mechanism, how the surface current density distribution on the proposed antenna varies with time has been investigated. Figure 6 presents the simulated surface current density distribution on the proposed antenna at the CP frequency of 5.6 GHz at four different times. In this figure, red arrows represent directions of the predominant surface current. When $t = 0$, the predominant surface current points to the right. When $t = T/4$, a downward directed predominant current is observed. It can be observed that the predominant current at $t = T/2$ ($3T/4$) is basically equal in magnitude and opposite in direction to that at $t = 0$ ($T/4$). As the time marches on, the predominant current turns in the clockwise direction in the azimuth plane. Hence, left-hand CP (LHCP) waves in the $+z$ axis direction can be excited, while the cross polarization is right-hand CP (RHCP).

3. SIMULATED AND MEASURED RESULTS

The proposed antenna in Figure 1 was fabricated and its reflection coefficients were measured using Agilent Vector Network Analyzer (E8361A). Figure 7 shows the simulated and measured S_{11} of the

proposed antenna. Simulated and measured results agree well with each other. The measured 10-dB impedance bandwidths are 2.39–2.54 GHz, 3.38–4.12 GHz, and 4.57–6.04 GHz, which fully cover all the 2.4 GHz (2.4–2.484 GHz)/5.2 GHz (5.15–5.35 GHz)/5.8 GHz (5.725–5.825 GHz) WLAN bands, all the 2.4 GHz (2.4–2.485 GHz)/5.5 GHz (5.15–5.85 GHz) Wi-Fi bands, and 3.5 GHz (3.4–3.69 GHz)/5.5 GHz (5.25–5.85 GHz) WiMAX bands. The slight discrepancies between the simulated and measured results may be caused by inevitable fabrication error and deviation between the actual relative permittivity and the one used in the simulation.

The AR, gain, and radiation pattern were measured using SATIMO system based on multiprobe technology in an anechoic chamber. The simulated and measured ARs in the $+z$ axis direction are shown in Figure 8. The measured 3-dB AR bandwidth of the proposed antenna is from 5.4 to 5.83 GHz, which fully covers 5.8 GHz WLAN band, partly covers 5.5 GHz Wi-Fi band and 5.5 GHz WiMAX band.

The performance of the proposed antenna is compared with other multi-band dual-polarized antennas in Table 2. Compared with the coaxial probe-fed antenna with six layer structure in [7], the proposed antenna is much simpler. The proposed antenna and the antennas in [8, 9] operate at close frequencies. However, the proposed antenna is simpler and more compact than the antennas in [8, 9].

Figure 9 presents the simulated and measured normalized far-field radiation patterns of the proposed antenna in zoy plane (E -plane) and zox plane (H -plane) at 2.45 and 3.5 GHz. It is clearly

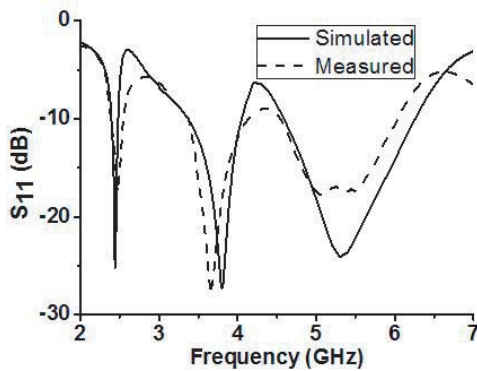


Figure 7. Simulated and measured S_{11} of the proposed antenna.

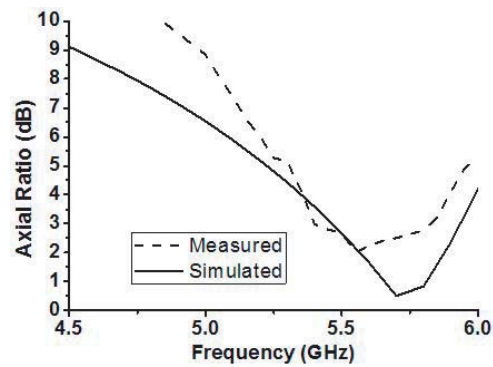


Figure 8. Simulated and measured AR results of the proposed antenna.

Table 2. Performance comparison for multi-band dual-polarized antennas.

antenna	10-dB impedance bandwidth	3-dB AR bandwidth	Overall dimension
antenna in [7]	1.215–1.241 GHz; 1.56–1.598 GHz; 1.78–1.83 GHz.	1.220–1.24 GHz 1.568–1.58 GHz	70 mm × 70 mm
antenna in [8]	1.92–2.17 GHz; 3.3–3.6 GHz; 5.1–5.3 GHz.	1.99–2.11 GHz	40 mm × 50 mm
antenna in [9]	2.28–2.5 GHz; 3.68–3.91 GHz; 5.67–8.25 GHz.	2.26–2.47 GHz	40 mm × 40 mm
proposed antenna	2.39–2.54 GHz; 3.38–4.12 GHz; 4.57–6.04 GHz.	5.4–5.83 GHz	25.35 mm × 29 mm

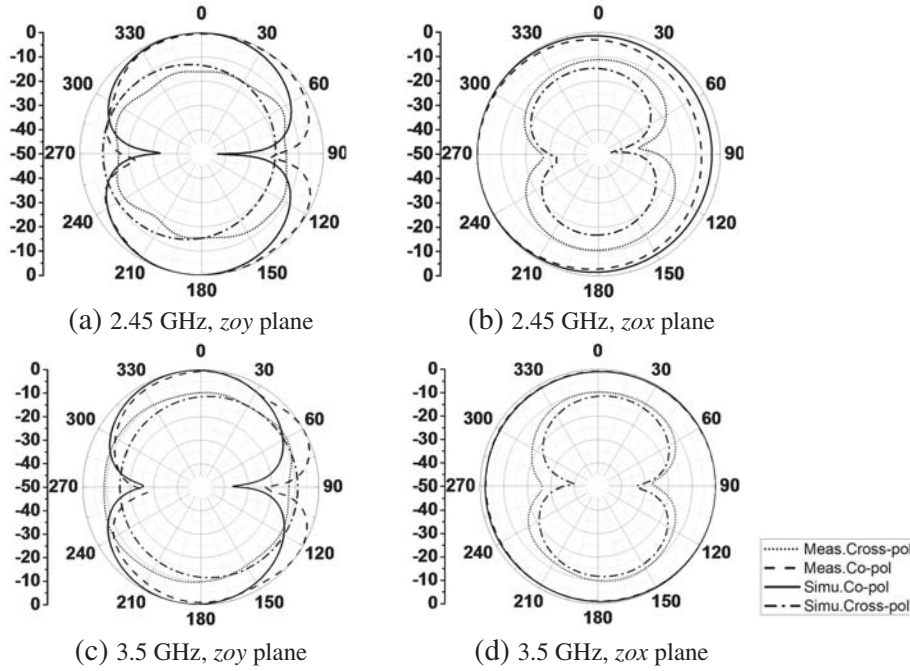


Figure 9. Simulated and measured radiation patterns of the proposed antenna at 2.45 and 3.5 GHz.

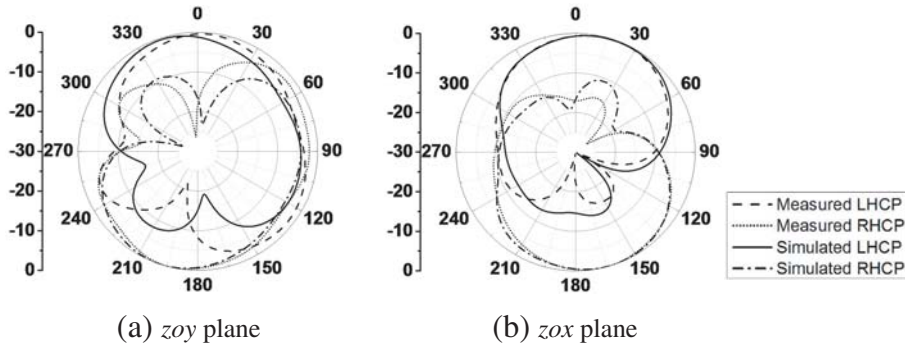


Figure 10. Simulated and measured radiation patterns of the proposed antenna at 5.5 GHz.

seen from Figure 9 that all the H -plane patterns exhibit a quasi-omnidirectional property and all the E -plane patterns have a quasi-“8” shape.

Figure 10 shows the simulated and measured normalized far-field radiation patterns of the proposed antenna in zoy and zox planes at the CP frequency of 5.5 GHz. It can be seen from Figure 10 that LHCP radiation power is much more than RHCP radiation power in the $+z$ axis direction. The measured gain of the proposed antenna varies from -1.56 to -0.45 dBi in the lower band, from 0.19 to 1.03 dBi in the middle band, from 2 to 3.04 dBi in the higher band.

4. CONCLUSION

In this paper, a compact tri-band dual-polarized planar monopole antenna with an asymmetrical ground plane and a loaded vertical stub is presented. The vertical stub is used for producing CP and asymmetrical ground plane for enhancing CP and especially impedance match performance. Its measured 10-dB impedance bandwidths are 2.39–2.54 GHz, 3.38–4.12 GHz, 4.57–6.04 GHz, which can fully cover all the 2.4/5.2/5.8 GHz WLAN bands, all the 2.4/5.5 GHz Wi-Fi bands, and 3.5/5.5 GHz WiMAX bands. Its measured 3-dB AR bandwidth can reach 430 MHz in the higher band. These good performances make it a very good candidate for practical Wi-Fi, WLAN/WiMAX applications.

ACKNOWLEDGMENT

This work was supported by the National Natural Science Foundation of China (Nos. 61331007 and 61361166008) and the Research Fund for the Doctoral Program of Higher Education of China (No. 20120185130001).

REFERENCES

1. Qian, K., C. Fan, and B. Wu, "Compact perturbed hexagonal microstrip antenna for dual-band circular polarization," *Electromagnetics*, Vol. 33, No. 8, 583–590, 2013.
2. Song, Y., Y.-C. Jiao, G. Zhao, and F.-S. Zhang, "Multiband CPW-fed triangle-shaped monopole antenna for wireless applications," *Progress In Electromagnetics Research*, Vol. 70, 329–336, 2007.
3. Chen, H., X. Yang, Y. Z. Yin, S. T. Fan, and J. J. Wu, "Triband planar monopole antenna with compact radiator for WLAN/WiMAX applications," *IEEE Antenn. Wirel. Propag. Lett.*, Vol. 12, 1440–1443, 2013.
4. Sze, J.-Y., T.-H. Hu, and T.-J. Chen, "Compact dual-band annular-ring slot antenna with meandered grounded strip," *Progress In Electromagnetics Research*, Vol. 95, 299–308, 2009.
5. Majid, H. A., M. K. Adb Rahim, M. R. Hamid, and M. F. Ismail, "Frequency reconfigurable microstrip patch-slot antenna with directional radiation pattern," *Progress In Electromagnetics Research*, Vol. 144, 319–328, 2014.
6. Row, J. S. and K. W. Lin, "Low-profile design of dual-frequency and dual-polarised triangular microstrip antennas," *Electronics Letters*, Vol. 40, No. 3, 156–157, 2004.
7. Falade, O. P., Y. Gao, and X. Chen, "Stacked-patch dual-polarized antenna for triple band handheld terminals," *IEEE Antenn. Wirel. Propag. Lett.*, Vol. 12, 202–205, 2013.
8. Mathew, S. and R. Anitha, "A compact tri-band dual-polarized corner-truncated sectoral patch antenna," *IEEE Trans. Antennas Propagat.*, Vol. 63, No. 12, 5842–5845, 2015.
9. Wang, Y. and X. Li, "Compact triple-band dual-polarized microstrip patch antenna for wireless applications," *Microwave Opt. Technol. Lett.*, Vol. 56, No. 4, 778–783, 2014.